Fastest growing linear Rayleigh-Taylor modes at solid/fluid and solid/solid interfaces

Guillermo Terrones
Applied Physics Division, Los Alamos National Laboratory, Los Alamos, New Mexico 87545, USA
(Received 10 August 2004; revised manuscript received 29 November 2004; published 18 March 2005)

Previous linear stability analyses of the Rayleigh-Taylor instability problem for elastic solids have been restricted to calculating the cutoff wavelength λ_c (zero growth rate) in the limit of Atwood number A of unity. Here, we rigorously derive the dispersion relations for solid/fluid and solid/solid interfaces and perform a systematic investigation to compute the most unstable modes (maximum growth rate) for all A. After rationalizing the dispersion relations into multivariable polynomials, we compute the physically meaningful wavelength λ and growth rate σ for all unstable disturbances as a function of the mechanical properties of the participating media (shear moduli, dynamic viscosity, and density contrast) and acceleration. It is shown that at these interfaces, the onset of instability can only arise via monotonically growing disturbances. For solid/fluid and solid/solid interfaces, the locus of the most unstable wavelength λ_m and growth rate σ_m pairs are calculated to cover the entire range of behavior in dimensionless space. We find that under certain conditions, at solid/fluid interfaces, two configurations with distinct A can have the same λ_m (a behavior that does not occur at solid/solid interfaces). In terms of estimating σ_m, λ_m, and λ_c, the applicability of our results extends to layers of finite thickness h provided $h > \lambda/2$. We suggest a plausible mechanism to explain the wavelength selection process in nominally smooth magnetically imploded liners observed in recent experiments.

DOI: 10.1103/PhysRevE.71.036306 PACS number(s): 46.25.Cc, 47.20.Bp, 46.90.+s, 68.35.Ja

I. INTRODUCTION

During the last 50 years, the Rayleigh-Taylor (RT) problem has been the subject of numerous theoretical, experimental, and numerical investigations. Most of these efforts have focused primarily on the problem of two Newtonian fluids of different thermophysical properties separated by an initially planar interface subjected to acceleration from the lighter toward the heavier fluid. A lucid conceptual presentation of the RT phenomenology was given by Sharp [1], who also posed important issues that remain relevant today (for a review on the Rayleigh-Taylor problem, the reader is referred to Kull [2]). In comparison to the vast amount of literature devoted to the RT problem for fluid/fluid interfaces, the number of papers dealing with RT instabilities in solids is very small.

Almost 40 years ago, Miles [3] performed the first theoretical study of the RT problem in an accelerated metal plate of infinite extent but finite thickness. The methodology proposed by Miles [3] for the analysis of RT instability in elastoplastic solids was adopted by several investigators [4–6] who elucidated some of the basic processes and principles that govern the growth of disturbances in these materials. This methodology was clearly presented by Robinson and Swegle [5], who also reviewed the work published by other authors before 1989. Bakhrakh and Kovalev [7,8] analyzed the linear stability of a metal/inviscid-fluid interface (see also Ref. [9]). Even though their work appeared in two papers (in Russian) in 1978 and 1980, it was not cited in the Western literature before 1993. In 1997, a report by Bakhrakh *et al.* [9] containing a compilation of Russian papers on the RT problem in solids became available in English. Using normal modes analysis for two-dimensional disturbances, Bakhrakh and Kovalev and Bakhrakh *et al.* [7–9] (BK) derived an equation for the growth rate as a function of wave number k. In the limit of a low-density fluid [i.e., Atwood number A of unity; $A=(\rho_{\text{solid}}-\rho_{\text{fluid}})/(\rho_{\text{solid}}+\rho_{\text{fluid}})$], they calculated the cutoff wavelength $\lambda_c(=2\pi/k_c)$ above which infinitesimal disturbances in the elastic solid would grow exponentially with time (metal plates accelerated by gas guns or high explosives can be adequately described within this limit). Drucker [10] applied the theory of perfectly plastic solids to determine the critical amplitude of a machined disturbance above which large plastic deformations occur in an accelerated metal half-space. In Drucker's approximate analysis [10], the critical amplitude is independent of the wavelength of the disturbance, an approximation that is applicable in the short-wavelength range [9].

The various analyses by the aforementioned investigators provided insights into and an understanding about the behavior of RT instabilities in elastoplastic solids. However, it was not until 1991 when the theoretical work of Nizovtsev and Raevskii [11] (NR) appeared that reasonable quantitative agreement with both numerical simulations [12] and experiments [13,14] was achieved [9,15]. NR followed an entirely different approach from that of Miles [3] and his followers [4–6] and Drucker [10]. They resorted to a combination of thin-plate theory, asymptotic matching, and physical insight that led to an equation relating the amplitude and wavelength of a machined disturbance together with the mechanical properties of the solid plate, its thickness, and acceleration (NR's work did not appear in Western literature until 1993 [15] and later in 1997 [9]). The first ingredient in the NR analysis required an expression for λ_c during the elastic growth of disturbances in a plate of finite thickness (for $A=1$). They derived an approximate relationship, within the elastic limit, that turned out to be reasonably accurate when compared to the exact solution derived seven years later by Plohr and Sharp (PS) [16] (the error in their λ_c, which is a function of layer thickness and driving parameters, is within 12%). For the problem of an accelerated elastic finite thick-

ness plate (for $A=1$), PS derived an exact analytic expression for the dispersion relation (in implicit form) and from it the cutoff wavelength. PS approached the RT analysis by recasting the governing equations into an initial/boundary value problem and then applying the Laplace transform method to find an analytic solution for the stream function. The NR stability boundary for the onset of plastic flow seems reasonably to agree with some experiments in metals accelerated by high explosives [9,13,14], although, as pointed out by Dimonte [17], it is not clear what the actual values for the mechanical properties are at these extreme conditions. Using a carefully characterized soft solid in which the mechanical properties were measured independently from the experiment, Dimonte *et al.* [18] performed experiments to determine the onset of RT instability. On average, the NR theory agrees with these experiments [18] to within 20% (ranging from 3% to 37% over eight experiments).

An area of active research at Los Alamos National Laboratory is the experimental and theoretical development of equations of state (EOS) for a variety of metals subjected to very high strain rates exceeding the levels reached by today's two-stage gas guns (less than 1 TPa impact pressure). Ultrahigh strain rates can be reached by magnetic implosion of impactor liners on targets that could develop pressures as high as 10 TPa, and peak accelerations could be as high as 10^{10} m/s^2 [19,20]. One concern during tests of this nature is the distortion of the impactor before it collides with the target sample to be studied, which would adversely affect experimental measurements. Reinovsky *et al.* [20] conducted the first experimental confirmation of RT instability growth in magnetically imploded aluminum cylindrical shells (nominally smooth and with machined disturbances). As pointed out by Keinigs *et al.* [19], liner design is an important component in developing successful EOS measurements using magnetic implosion. These authors [19] have discussed the advantages of using composite impactor liners with an inner layer of tungsten and an outer layer of aluminum, particularly in the TPa range. The ideal high-performance liner design would prevent instability feedthrough [19] by precluding the imprinting of instabilities in the outer layer to be transferred to the inner region of the liner. Depending on a particular liner design, instability feedthrough could occur when disturbances in the outer layer of the shell grow substantially during implosion [21]. At some stage in this process, before impacting the target, the entire liner could remain as a solid, a molten metal, or a combination of solid and melt. In this situation, there are two interfaces that could give rise to RT instabilities, namely the liquid layer with a massless medium and the solid adjacent to the liquid metal. If the initial disturbances in the liner have large amplitude, feedthrough could occur before melting [20]. If a liner design were as smooth as it could possibly be manufactured, the imperfection amplitudes and wavelength could lie on the stable side of the stability boundary leading to no growth of disturbances, provided the liner retained its strength as it implodes. However, typical magnetic driving conditions [20] could be sufficiently high to cause thermal softening and/or melting of the outer layer (in either a uniform or composite liner shell), a few microseconds after implosion is initiated, making it susceptible to RT instabilities and possible feedthrough to the inner layer of the liner [19].

If high temperatures were reached without melting in a composite liner design, thermal softening would effectively reduce the shear moduli of the metal layers. Absent melting, a sufficiently softened metal/metal interface could also be susceptible to growth of elastic instabilities whose length scales are comparable to the characteristic dimensions of the liner. To the best of the author's knowledge, the stability of solid/solid interfaces has not been studied previously. The shear modulus decreases linearly with increasing temperature and can reach very low values near the melting point. Numerical simulations of imploding liners have shown that the wavelength of imprinted disturbances differs significantly from the evolving disturbances that grow at the outer region of the molten layer [19]. Therefore, knowledge about the nature of the growth of disturbances at solid/fluid and solid/solid interfaces will aid in our understanding of instability feedthrough. It is also important to discern among the spectrum of unstable disturbances which ones will have the *fastest rate of growth* at a specific interface.

The scope of previous linear stability analyses at metal/fluid interfaces was narrow in that they were restricted to $A=1$, focused on the cutoff wavelength to establish the instability criteria, and a systematic investigation to identify and calculate the fastest-growing disturbances together with their dependence on the driving parameters was not conducted. At a solid-metal/molten-metal interface, not only is $A\neq 1$, but also the viscosity of the melt may not be neglected at sufficiently high accelerations, especially if the adjoining metal has softened considerably. In fact, as shown in this paper, viscosity and the degree of softening affect the selection of the wavelengths that lead to the fastest-growing disturbances. Here we consider the linear stability of disturbances at two different kinds of interfaces, namely a linear-elastic-solid/viscous-liquid and between two different linear-elastic-solids, and after rationalizing the dispersion relations, we derive exact relationships in the form of multivariable polynomials with which the instability loci for the most unstable disturbances can be determined.

The paper is organized as follows. First, we present the governing equations and derive the dispersion relations from the linearized disturbance equations for solid/fluid and solid/solid interfaces. We discuss our analytical approach to the problem, based on the rationalization of the dispersion relations by dialytic elimination [22,23]. This is followed by a presentation of the results and a brief discussion about the relationship of our analyses with recent experiments [20].

II. FORMULATION AND LINEAR STABILITY ANALYSES

A. Solid/fluid interface

We consider a layer of an incompressible Hookean solid overlying a layer of a Newtonian incompressible fluid. These continuous media lie on opposite sides of an initially planar interface located at $z=0$. The fluid 1 and the solid 2 occupy the domains $-\infty<z\leqslant 0$ and $0\leqslant z<\infty$, respectively, and have densities ρ_1 and ρ_2. To allow for a general derivation, the shear modulus G of the solid, the dynamic viscosity μ of the

fluid, and both densities are all functions of z. The media are subjected to a steady, uniform acceleration $\mathbf{a}=-a\mathbf{e}_z$ perpendicular to the initial interface.

The momentum equation in Cartesian coordinates in a Eulerian reference frame for a continuum medium is

$$\rho\left(\frac{\partial U_i}{\partial t}+U_j\frac{\partial U_i}{\partial x_j}\right)=-\frac{\partial P}{\partial x_i}+\frac{\partial S_{ij}}{\partial x_j}+\rho a_i, \tag{1}$$

where ρ is the density of the medium, t is the time variable, x_i are the coordinate directions ($x_1=x$, $x_2=y$, $x_3=z$), U_i are the corresponding velocity components, P is the hydrostatic pressure, S_{ij} are the components of the deviatoric stress tensor, and a_i are the acceleration components. For a Hookean solid, the constitutive equation is

$$\frac{\partial S_{ij}}{\partial t}=G\left(\frac{\partial U_i}{\partial x_j}+\frac{\partial U_j}{\partial x_i}\right). \tag{2}$$

Conservation of mass requires that

$$\frac{\partial U_i}{\partial x_i}=0, \tag{3}$$

and to ensure the constancy of the density of individual particles during motion [24],

$$\frac{\partial \rho}{\partial t}+U_i\frac{\partial \rho}{\partial x_i}=0. \tag{4}$$

For a Newtonian fluid, the constitutive equation is

$$S_{ij}=\mu\left(\frac{\partial U_i}{\partial x_j}+\frac{\partial U_j}{\partial x_i}\right). \tag{5}$$

Chandrasekhar [24] studied the linearized RT instability at a fluid/fluid interface, and more recently, Mikaelian [25] generalized the analysis to layers of finite thickness. In the case of Hookean solids, the derivation of the linearized perturbation equations is analogous to that for fluids [24], and some details will be omitted. To carry out a normal modes analysis, it is assumed that disturbances occur in the x-y plane and are superimposed to the motionless basic state according to

$$\begin{Bmatrix} U_i \\ P \\ \rho \\ S_{ij} \end{Bmatrix} = \begin{Bmatrix} 0 \\ \overline{p}(z) \\ \overline{\rho}(z) \\ 0 \end{Bmatrix} + \varepsilon \begin{Bmatrix} u_i(z) \\ p(z) \\ \delta(z) \\ s_{ij}(z) \end{Bmatrix} \exp[\sigma t + i(k_x x + k_y y)], \tag{6}$$

where σ is the disturbance growth rate; k_x and k_y are the wave numbers for disturbances that propagate horizontally; $u_i(z), p(z), \delta(z)$, and $s_{ij}(z)$ are disturbance amplitudes for the velocity, pressure, density, and stress, respectively; the bar denotes the basic state; and $\varepsilon \ll 1$. Because of the horizontal isotropy in this geometry, two-dimensional disturbances need only be considered with a wave number k defined by $k=(k_x^2+k_y^2)^{1/2}$. The linearized perturbation equations are obtained upon substitution of Eq. (6) into Eqs. (1)–(4) and neglecting terms of $O(\varepsilon^2)$ and higher. After some algebra, it can be shown that these equations can be reduced to a single ordinary differential equation for the velocity disturbance $w(z)[=u_3(x_3)]$ in the vertical direction

$$Gw^{(iv)}+2G'w^{(iii)}-(2k^2G-G''+\sigma^2\overline{\rho})w''-(2k^2G'+\sigma^2\overline{\rho}')w'+k^2(k^2G+G''-a\overline{\rho}'+\sigma^2\overline{\rho})w=0, \tag{7}$$

where the prime denotes derivative with respect to z. Hereafter, we specialize the analysis to the case in which the mechanical properties in both the fluid and solid layers are constant. This and the boundary conditions at infinity $w(z\to\pm\infty)=0$ simplify the general solution of Eq. (7) (and its counterpart for the fluid region). Upon application of the kinematic and dynamic conditions at the solid/fluid interface, a linear system of equations in the amplitude of the disturbances is obtained. By requiring that nontrivial solutions exist, the characteristic equation (dispersion relation) $C_{sf}(\rho_1,\rho_2,\mu,G,a,k,\sigma)=0$ that relates the growth rate, the wave number of disturbances, and the controlling parameters is obtained. In terms of dimensionless variables, the dispersion relation can be written as

$$C_{sf}(r,m,\kappa,\alpha)=F_1(r,\kappa,\alpha)+\frac{m}{\beta_1}F_2(r,m,\kappa,\alpha)=0, \tag{8}$$

where the dimensionless variables are $\alpha^2=(\sigma/a)^2G/\rho_2$, $\kappa=Gk/(\rho_2 a)$, $r=\rho_1/\rho_2$, $m^2=a\mu(\rho_2/G^3)^{1/2}$, $\beta_1=(r\alpha+m^2\kappa^2)^{1/2}$, $\beta_2=(\alpha^2+\kappa^2)^{1/2}$, and the functions $F_1(r,\kappa,\alpha)$ and $F_2(r,m,\kappa,\alpha)$ are given by

$$F_1=(1+r)\alpha^4-(1-r-4\kappa)\kappa\alpha^2+4(\kappa-\beta_2)\kappa^3, \tag{9}$$

$$F_2=r(1+r)\beta_2\alpha^4-(1-r)[(1-r)\alpha^2+r\beta_2]\kappa\alpha^2+\{1-r^2-4[m\alpha\beta_1+r(1-m^2\alpha)\beta_2]\}\kappa^2\alpha^2+4[\beta_2-m\alpha(2-m^2\alpha)\times(\beta_1+m\beta_2)]-4(1-m^2\alpha)^2\kappa^5-4[(1-r)(1-m^2\alpha)\alpha-m(2-m^2\alpha)\beta_1\beta_2]\kappa^3\alpha. \tag{10}$$

If the fluid layer is inviscid, then $m=0$, and Eq. (8) becomes $F_1=0$ and is equivalent to the characteristic equation derived by Bakhrakh and Kovalev and Bakhrakh *et al.* [7–9] (BK) in dimensional form (after the substitution $a=-g$). Robinson and Swegle [5] arrived at an equation similar to Eq. (9) but with $r=0$.

B. Solid/solid interface

For a solid/solid interface, we consider two layers of incompressible Hookean media lying on opposite sides of an initially planar interface located at $z=0$. Solids 1 and 2 occupy the domains $-\infty<z\leqslant 0$ and $0\leqslant z<\infty$, respectively, and have densities ρ_1 and ρ_2 and shear moduli G_1 and G_2. As before, both solids are subjected to a steady, uniform acceleration $\mathbf{a}=-a\mathbf{e}_z$ perpendicular to the initial interface. In this case, Eq. (7) is applied to both sides of the interface, assuming that the mechanical properties are constant. Enforcing the appropriate boundary conditions and the conditions at the solid/solid interface leads to the dispersion relation $C_{ss}(\rho_1,\rho_2,G_1,G_2,a,k,\sigma)=0$, which in dimensionless form is

$$C_{ss}(r,R,\kappa,\alpha) = F_1(r,\kappa,\alpha) + \frac{R}{\beta_3}F_3(r,R,\kappa,\alpha) = 0, \quad (11)$$

where $R^2 = G_1/G_2$, $\beta_3 = (r\alpha^2 + R^2\kappa^2)^{1/2}$, $F_1(r,\kappa,\alpha)$ is given by Eq. (9), and $F_3(r,R,\kappa,\alpha)$ is

$$\begin{aligned} F_3 = {} & r(1+r)\beta_2\alpha^4 - (1-r)[(1-r)\alpha^2 + r\beta_2]\kappa\alpha^2 + \{1 - r^2 \\ & - 4[R\beta_3 + r(1-R^2)\beta_2]\}\kappa^2\alpha^2 + 4[(1-R^2)^2\beta_2 - R(2 \\ & - R^2)\beta_3] - 4(1-R^2)^2\kappa^5 - 4[(1-r)(1-R^2)\alpha^2 - R(2 \\ & - R^2)\beta_2\beta_3]\kappa^3. \end{aligned} \quad (12)$$

If the lighter medium has no strength ($G_1 = 0$), Eq. (11) reduces to the same limit as that of Eq. (8) for a solid/fluid interface in which the fluid region is inviscid ($\mu = 0$).

III. ANALYTICAL APPROACH

A. Cutoff wave numbers

For a given set of controlling parameters in either a solid/fluid or a solid/solid interface, the nature of the disturbances is specified by their growth rate through the dispersion relations $C_{sf}(r,m,\kappa,\alpha) = 0$ and $C_{ss}(r,R,\kappa,\alpha) = 0$, Eqs. (7) and (11), respectively. Disturbances that neither grow nor decay are neutral ($\alpha = 0$) and demarcate the stability boundary corresponding to the cutoff perturbations of dimensionless wave number κ_c. Thus, disturbances whose wave numbers are in the range $0 \leqslant \kappa < \kappa_c$ are unstable, and within this range there will be a disturbance with a maximum growth rate, i.e., the fastest growing in the linear regime. For a solid/fluid interface, a general expression for κ_c can be determined by expanding Eq. (8) as a Taylor series around $\alpha = 0$,

$$\frac{2mC_{sf}}{r\alpha^3} = 2\kappa + r - 1 + O(\alpha),$$

therefore the dimensionless cutoff wave number is

$$\kappa_c = \frac{1-r}{2} = \frac{A}{1+A}, \quad (13)$$

where $A = (1-r)/(1+r)$ and κ_c is a function of the density ratio only. In terms of dimensional variables,

$$k_c = \frac{(\rho_2 - \rho_1)a}{2G}, \quad (14)$$

which is the result derived by previous authors [7–9,16]. Those authors arrived at the above result under the assumption that $A = 1$ (or $r = 0$), but this approximation is not necessary. Similarly, for a solid/solid interface, the leading-order expansion of Eq. (11) in α is

$$\frac{2RC_{ss}}{r(1+R^2)\alpha^4} = 2(1+R^2)\kappa + r - 1 + O(\alpha)$$

and

$$\kappa_c = \frac{1-r}{2(1+R^2)} = \frac{A}{(1+A)(1+R^2)}. \quad (15)$$

Therefore, for a solid/solid interface, κ_c is both a function of the density ratio and of the shear moduli ratio R. The dimensional version of Eq. (15) for the cutoff wave number is

$$k_c = \frac{(\rho_2 - \rho_1)a}{2(G_1 + G_2)}. \quad (16)$$

It is important to note that for a solid/fluid interface, k_c does not involve the viscosity of the fluid that "pushes" against the solid, whereas for a solid/solid interface, k_c is a function of the mechanical properties of both materials.

B. Most unstable disturbances

Solid/fluid and solid/solid interfaces will have the same stability behavior provided the fluid is inviscid in the former and the lighter solid has no shear strength in the latter. Therefore, when inertia is the determining factor that characterizes the behavior of the lighter layer, then $C_{sf}(r,0,\kappa,\alpha) = C_{ss}(r,0,\kappa,\alpha)$, in which case the characteristic equation is $F_1(r,\kappa,\alpha) = 0$. For this limiting case, it will be shown that exact analytic solutions can be deduced for the fastest growing disturbances for all Atwood numbers. The importance of a systematic analysis within this limit is twofold. First, it shares distinctive features with the stability and growth of disturbances for the general cases (i.e., when the shear stresses within the lower layer cannot be neglected in either solid/fluid or solid/solid interfaces). Second, the mathematical methodology for the treatment of the dispersion relation, which carries over the general cases, can be presented in detail. Thus, we begin by examining the stability of interfaces governed by Eq. (9).

From the point of view of analysis, one difficulty in dealing with these kinds of dispersion relations lies in the fact that both of the dimensionless variables of interest, i.e., the growth rate and wave number, appear as sums raised to a noninteger power. Equations (8) and (11) contain linear combinations of the unrationalized terms $\beta_1, \beta_2, \beta_3, \beta_1\beta_2$, and $\beta_2\beta_3$. Rationalization of the dispersion relation allows for an analytic treatment of the stability boundary in terms of multivariable polynomial equations. Within this framework, it can readily be established whether or not the onset of instability is through monotonically or oscillatory growing disturbances because the dispersion relation can be written in the form

$$H_1(r,\phi,\omega,\kappa) + i\omega H_2(r,\phi,\omega,\kappa) = 0, \quad (17)$$

where H_1 and H_2 are real-valued polynomials, ϕ could be either m or R, and the oscillation frequency of disturbances ω is related to the growth rate through $\alpha = i\omega$. For there to be oscillatory onset, H_2 must exist, the roots of $H_2 = 0$ must be positive real numbers [$\mathrm{Im}(\omega) = 0$ and $\omega > 0$], and for those roots to be physically meaningful they must satisfy the unrationalized dispersion relation. If these conditions are not satisfied, then the system can only become unstable via monotonically growing disturbances (steady onset).

We proceed to rationalize Eq. (9) (which contains a single unrationalized term, i.e., β_2) to transform it into a polynomial in α, κ, and r. A general procedure for the rationalization of equations is by dialytic elimination of the radical terms through the computation of Sylvester's resultant

[22,23]. We denote the rationalized form of $F_1(r,\kappa,\alpha)=0$, after eliminating β_2, as $f_1(r,\kappa,\alpha)=0$, which can be written as

$$f_1 = \alpha^6 - \frac{2(1-r-4\kappa)\kappa}{1+r}\alpha^4 + \left\{\left(\frac{1-r}{1+r}\right)^2 - 8\left[\frac{1-r-(3+r)\kappa}{(1+r)^2}\right]\kappa\right\}\kappa^2\alpha^2 - \frac{8(1-r-2\kappa)}{(1+r)^2}\kappa^5 = 0. \tag{18}$$

In rationalized form, the characteristic equation is transformed into a multivariable polynomial that is cubic in α^2 and from its discriminant it can be shown that there is only one real root that corresponds to the physically meaningful solution for the growth rate. The interface will be unstable for all configurations that lead to values of $\alpha^2>0$, neutrally stable for $\alpha^2=0$, and stable otherwise. Since Eq. (18) only has even powers of α, this implies that H_2 in Eq. (17) is identically zero, and thus oscillatory onset is not possible in this system.

The most unstable disturbances are those with a maximum value of α^2 in the α-κ plane and thus satisfy $\partial\alpha^2/\partial\kappa=0$. Therefore, a relationship that is satisfied at the maximum value of the growth rate α_m corresponding to a wave number κ_m is obtained by implicit differentiation of $f_1(r,\kappa,\alpha)=0$ with respect to κ, solving for $\partial\alpha^2/\partial\kappa$, and equating to zero,

$$(1-r-8\kappa)\alpha^4 - \left\{\frac{(1-r)^2}{1+r} - 4\left[\frac{3(1-r)-4(3+r)\kappa}{1+r}\right]\kappa\right\}\kappa\alpha^2 + 4\left[\frac{5(1-r)-12\kappa}{1+r}\right]\kappa^4 = 0. \tag{19}$$

After dialytically eliminating α^2 from Eqs. (18) and (19), a quartic equation for the most unstable dimensionless wave number κ_m is obtained, which in terms of the Atwood number becomes

$$[11+A(3+8A)]\kappa_m^4 + \frac{A[9-A(7+32A)]}{2(1+A)}\kappa_m^3 + \frac{A^2(3+50A)}{4(1+A)}\kappa_m^2 - \frac{3A^3(9+10A)}{8(1+A)^2}\kappa_m + \frac{3A^4}{8(1+A)^2} = 0. \tag{20}$$

Similarly, κ can be eliminated between Eqs. (18) and (19),

$$[11+A(3+8A)]^2\alpha_m^8 - \frac{A^2[63+3A(156+157A)+2A^3(9+8A)]}{1+A}\alpha_m^6 + \frac{A^4(486+873A+4A^3)}{4(1+A)}\alpha_m^4 - \frac{27A^6(19+20A)}{16(1+A)^2}\alpha_m^2 + \frac{27A^8}{16(1+A)^2} = 0, \tag{21}$$

resulting in a quartic polynomial in α_m^2. The departure from the classical RT growth rate (i.e., for inviscid fluids) can be quantified by the ratio $\eta_m=\alpha_m/(A\kappa_m)^{1/2}[=\sigma_m/(Aa\kappa_m)^{1/2}]$ for which an equation can be found readily from Eqs. (18) and (19),

$$(11+3A+8A^2)\eta_m^8 - 2(15-5A+4A^2)\eta_m^6 + (39-12A+2A^2)\eta_m^4 - \frac{3}{2}(15-2A)\eta_m^2 + \frac{9}{2} = 0. \tag{22}$$

To rationalize the entire characteristic equation (8), two separate dialytic eliminations are necessary to eliminate β_1 and β_2. At each elimination step, the order of the multivariable polynomials and the number of independent terms increases. Let us denote a dialytic elimination step between two expressions by $\mathcal{D}\{\cdot,\cdot\}$ and the unrationalized term ξ to be eliminated is denoted by a superscript in parentheses $C_x^{(\xi)}(x=sf,ss)$. For a solid/fluid interface, the steps required for rationalization to eliminate β_1 and β_2 are

$$C_{sf}^{(\beta_1)} = \mathcal{D}\{C_{sf}, r\alpha + m^2\kappa^2 - \beta_1^2\}, \tag{23}$$

$$C_{sf}^{(\beta_1,\beta_2)} = \mathcal{D}\{C_{sf}^{(\beta_1)}, \alpha^2 + \kappa^2 - \beta_2^2\}, \tag{24}$$

which yield a 14th-order multivariable polynomial in α,

$$C_{sf}^{(\beta_1,\beta_2)} = \sum_{n=0}^{14} q_n(r,m,\kappa)\alpha^n = 0, \tag{25}$$

where q_n is the nth coefficient of the rationalized dispersion relation (the explicit form of each q_n is not transcribed here because the expressions are considerably long). Substituting $\alpha=i\omega$ in Eq. (25) leads to

$$\sum_{n=0}^{7} qr_n(r,m,\kappa)\omega^{2n} + i\omega\sum_{n=0}^{6} qi_n(r,m,\kappa)\omega^{2n} = 0, \tag{26}$$

where qr_n and qi_n are the coefficients for the real and imaginary parts of the dispersion relation, respectively. Even though the H_2 polynomial in ω [see Eq. (17)] exists, the roots of $H_2=0$ from Eq. (26) are not physically meaningful, and thus there is no oscillatory onset. This is not a surprising result because in neither the fluid/fluid nor in the solid/vacuum systems is oscillatory onset possible, as shown by Menikoff *et al.* [26] and by PS [16], respectively. For a solid/solid interface, two rationalization steps are needed as well,

$$C_{ss}^{(\beta_2)} = \mathcal{D}\{C_{ss}, \alpha^2 + \kappa^2 - \beta_2^2\}, \tag{27}$$

$$C_{ss}^{(\beta_2,\beta_3)} = \mathcal{D}\{C_{ss}^{(\beta_2)}, r\alpha^2 + R^2\kappa^2 - \beta_3^2\}, \tag{28}$$

to yield a polynomial in even powers of α,

$$C_{ss}^{(\beta_2,\beta_3)} = \sum_{n=0}^{6} Q_n(r,R,\kappa)\alpha^{2n} = 0, \tag{29}$$

where Q_n is the nth coefficient of the rationalized dispersion relation. Since Eq. (29) has no imaginary part, i.e., H_2 is identically zero, only monotonically growing disturbances are physically meaningful at the onset of instability.

IV. RESULTS

We begin this section with the interfacial stability of a solid overlying a layer that possesses inertia without viscos-

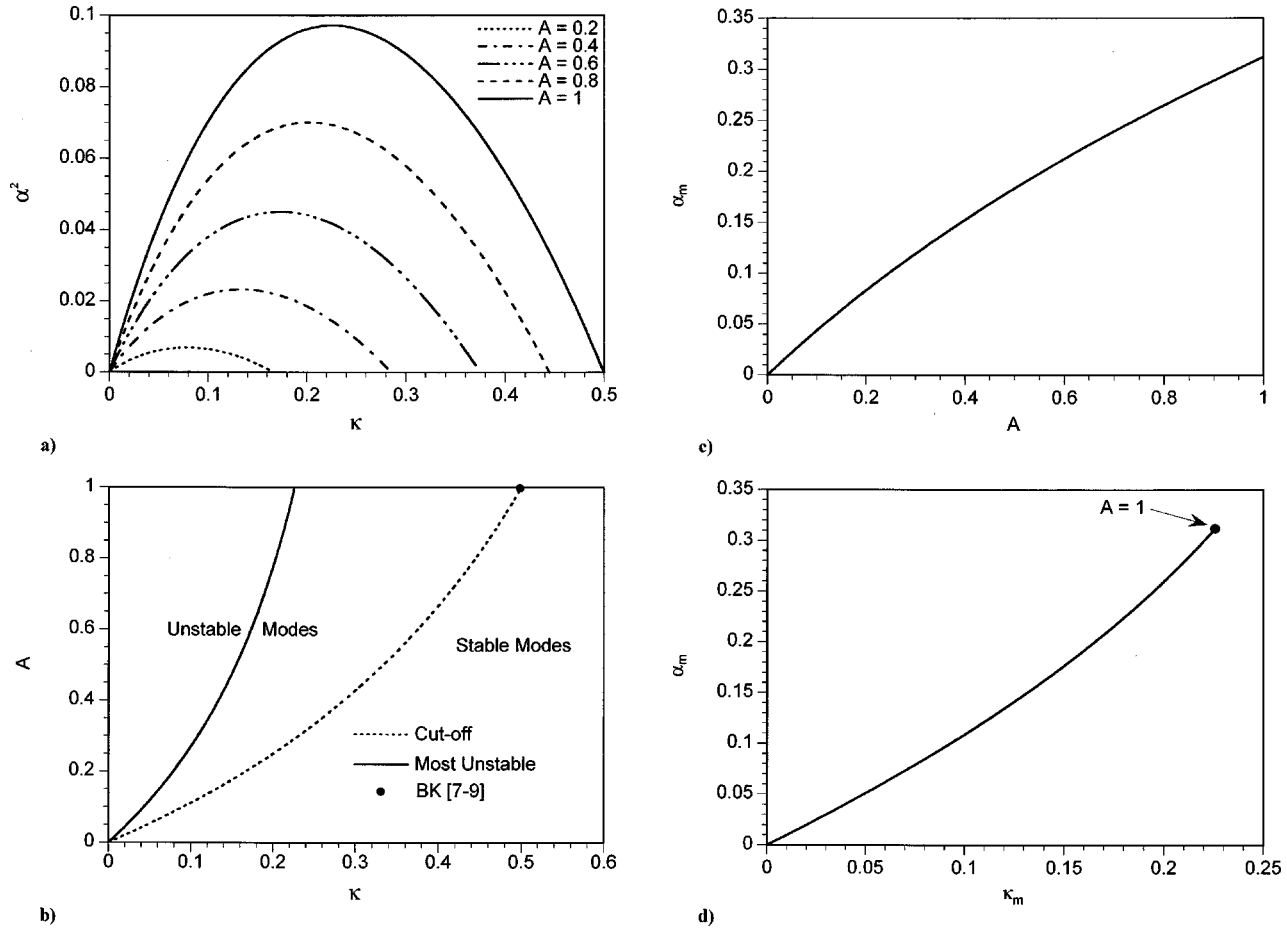

FIG. 1. For $C_{sf}=C_{ss}$, (a) variation of α^2 as a function of κ for different values of A: —, $A=1$; - - - - - -, $A=0.8$; —···—,$A=0.6$; –·–·–·–, $A=0.4$; ·····A,=0.2. (b) Stability boundary in the A-κ plane: —, κ_m; ·····κ_c. (c) Variation of the maximum dimensionless growth rate α_m as a function of A. (d) Maximum dimensionless growth rate α_m as a function of the most unstable dimensionless wave number κ_m for all A.

ity ($m=0$) or strength ($R=0$). This is followed by results for the stability of solid/fluid and solid/solid interfaces with microscopic physics (i.e., viscosity and strength) at both sides of the interface, where the effects that the controlling dimensionless parameters have on the stability boundary and growth rate of disturbances are explored over the entire range of behavior in the dimensionless parameter space. The availability of efficient variable-precision-arithmetic algorithms for the numerical solution of algebraic polynomial equations of high order makes the computation of the growth rates α as a function of wave number κ (and the driving parameters) for the systems considered here expedient. This approach avoids potential difficulties encountered in the numerical solution of systems of unrationalized equations [such as $C_{sf}(r,m,\kappa,\alpha)=0$ and $\partial C_{sf}(r,m,\kappa,\alpha(\kappa))/\partial\kappa=0$] by Newton iteration when the radii of convergence are very small.

For $m=0$ (or equivalently $R=0$), since all of the equations for α and the most unstable κ are fourth order or less, closed-form solutions were used to compute the locus of the most unstable modes as a function of Atwood number A. Figure 1(a) shows the variation of α^2 as a function of κ for different values of A obtained from the physically meaningful solution of Eq. (18). For a given configuration, the interface will be unstable for all values of κ such that $\alpha^2>0$, neutrally stable for $\kappa=\kappa_c$ [given by Eq. (13)] when $\alpha^2=0$, and stable otherwise. We note that in the limit $A=1$, our analytical result of $\kappa_c=1/2$ [where the solid curve in Fig. 1(a) intercepts the abscissa] agrees with the result obtained by BK and with that of PS in the limit of large h. Miles' result of $\kappa_c=4/13$ [3] is smaller than the correct answer by a factor of 1.625. As pointed out earlier [9,11,16], the approach taken by Miles [3] and his followers [4–6] is flawed because for solids the velocity field cannot be correctly approximated by the stream function of an inviscid flow. The κ of the most unstable disturbance κ_m lies within the range $0<\kappa_m<\kappa_c$ and occurs when α^2 has a maximum denoted by α_m^2. Physically, this condition takes place when the inertial forces, buoyancy forces, and the stabilizing forces due to the strength of the solid are of comparable magnitude. The upper bound on the most unstable growth rate occurs when $A=1$ [solid curve in Fig. 1(a)], for which $\alpha_m^2=0.0972(\alpha_m=0.3118)$ and $\kappa_m=0.2256$. At first glance, the growth rate curves appear to be symmetric with respect to κ_m, but as seen in Fig. 1(b), κ_m is always less than half of κ_c for a fixed A. As the density contrast decreases, both α_m and κ_m monotonically decay to zero, thus to effect destabilization, disturbances with increasingly large wavelengths are required. This is clearly illustrated in Fig. 1(b), which shows the stability boundary κ_c

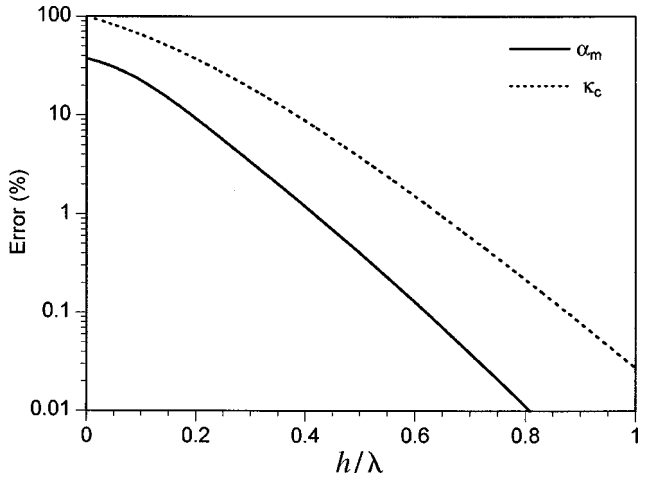

FIG. 2. Error in α_m and κ_c as a function of h/λ when computed with the semi-infinite thickness layer theory: —, α_m; ·····, κ_c.

(dotted curve) and κ_m as a function of A, the latter of which was computed from Eq. (20). The dot in the upper right-hand corner of the dotted curve represents the result derived by BK. Figure 1(c) shows the growth rates for all A that lead to the most unstable configuration computed from Eq. (21) and Fig. 1(d) shows the dependence of α_m with κ_m.

In our linear stability analyses, there is no explicit length scale because the participating media extend to infinity in the direction of acceleration. To assess the applicability limits of our results to finite thickness layers, the values of α_m, κ_m, and κ_c computed from the dispersion relation derived by PS (valid only for $A=1, m=0$ [16]) as a function of the plate thickness h are compared to those obtained from Eqs. (13), (20), and (21) in the limit $A=1$. With the same definitions for the dimensionless growth rate and wave number used in Eq. (9) [$\alpha^2=(\sigma/a)^2 G/\rho$, $\kappa=Gk/(\rho a)$, and $\beta=(\alpha^2+\kappa^2)^{1/2}$], and introducing the dimensionless thickness $\theta=\rho a h/G$, PS's dispersion relation becomes

$$\alpha^4[\alpha^4-\kappa^2+8\kappa^2(\alpha^2+3\kappa^2)]+8\kappa^3\{2\kappa^3(3\alpha^2+2\kappa^2)-\beta(\alpha^2+2\kappa^2)^2\times[\coth(\theta\kappa)\coth(\beta\theta)-\operatorname{csch}(\theta\kappa)\operatorname{csch}(\beta\theta)]\}=0. \tag{30}$$

An expression for κ_c involving θ is obtained after dividing Eq. (30) by α^4 and then expanding in Taylor series around $\alpha=0$,

$$(1-4\kappa_c^2)\sinh^2(\theta\kappa_c)+(2\theta\kappa_c^2)^2=0. \tag{31}$$

For instance, if $h=0.4\,\lambda$, the errors in estimating α_m, κ_m, and κ_c are 1.2%, 2.1%, and 8.9%. If $h>\lambda/2$, the corresponding errors for α_m, κ_m, and κ_c are less than 0.5%, 1.3%, and 3.8%, respectively. The largest error is always on κ_c for all h/λ_c. As shown in Fig. 2, for α_m and κ_c, this error drops almost exponentially as h/λ increases (the error in κ_m is either between κ_c and α_m or less than that for α_m if $0.19<h/\lambda<0.35$). This is a reflection of the fact that only a small distance away from the interface influences the linear instability growth in all RT configurations, regardless of whether they are solid or fluid. NR relied on this fact to approximate κ_c as a function of h. Even though the percentage error comparisons in Fig. 2 are for the case $A=1$ and $m=0$ (or $R=0$), similar trends are expected in the case of an interface with two distinct participating media (i.e., $A\neq 1$, $m\neq 0$, $R\neq 0$).

The departure from the classical growth rate for $m=0$ (or $R=0$) is found by solving Eq. (22), whose solution is approximately given by

$$\eta_m \approx 0.666(1-0.024A+0.0096A^2). \tag{32}$$

Thus, for all of the possible most unstable configurations the mean value of $\eta_m[=\alpha_m/(A\kappa_m)^{1/2}=\sigma_m/(Aa\kappa_m)^{1/2}]$ is 0.67. From Eq. (32), an approximate expression (leading order in A) for the growth rate in terms of dimensional variables is obtained,

$$\sigma_m \approx 0.67\sqrt{Aak_m}, \tag{33}$$

where $k_m \approx (0.478-0.027A)k_c$. Interestingly, the growth rate estimated by Drucker for the amplitude of a machined sinusoidal disturbance, of wave number k, in a perfectly plastic solid half-space is $0.674\sqrt{ak}$ [10], provided the initial preformed disturbance amplitude exceeds $2Y/\rho a$ (Y is the yield stress of the solid in uniaxial tension) [10].

For a solid/fluid interface, with a fixed A(=0.8), Fig. 3(a) shows α^2 as a function of κ for increasing values of m as obtained from the physically meaningful solutions of Eq. (25). In an actual system, the parameter m increases with viscosity ($\sim\mu^{1/2}$) and decreases with shear modulus ($\sim G^{-3/4}$). Since κ_c is only a function of A [see Eq. (13)], all of the curves in Fig. 3(a) have the same κ_c. As m increases, the maximum shifts towards smaller κ while the growth rate rapidly decays towards zero for wave numbers larger than κ_m. In the neighborhood of κ_c, the growth-rate curves behave like $\alpha^2\sim 1/m^4$. This rapid decay requires that for $m>0$, there must be an inflection point for $\kappa>\kappa_m$. As expected, for very small κ, the growth rate is linear and weakly dependent on the microphysics. For a fixed m(=1), Fig. 3(b) shows α^2 as a function of κ for different values of A. As in Fig. 3(a), there is also an inflection point, but in this case, it is increasingly closer to the interception with the abscissa as A decreases. Figure 3(c) shows that for a fixed A, as m increases, longer wavelengths are needed to achieve the most unstable mode, even though the critical wavelength remains the same [see Fig. 3(a)]. For large values of m, Fig. 3(c) shows that κ_m becomes weakly dependent on the density contrast, while for small values of A, κ_m is weakly dependent on m. Figure 3(d) shows the locus of the most unstable α_m-κ_m pairs for all A and different m. The dots denote configurations where $A=1$, and below this point A decreases monotonically to zero at the origin. For $m\geqslant 2.1$, there is a point of infinite slope ($\partial\alpha_m/\partial\kappa_m=\infty$), which for $m=2.1$ occurs at $A=1$. This implies that for $m>2.1$, curves in the α_m-κ_m plane are double-valued over a small range of κ_m. Therefore, for a fixed m such that $m>2.1$, there are two configurations (with different A) whose most unstable wave number is identical and their respective growth rates are different. For instance, if $m=50$, the interfaces with $A=0.64$ and $A=0.937$ have the same $\kappa_m=0.002\,682$. Figure 3(e) shows the double-valued region in the α_m-κ_m plane for $m=50$.

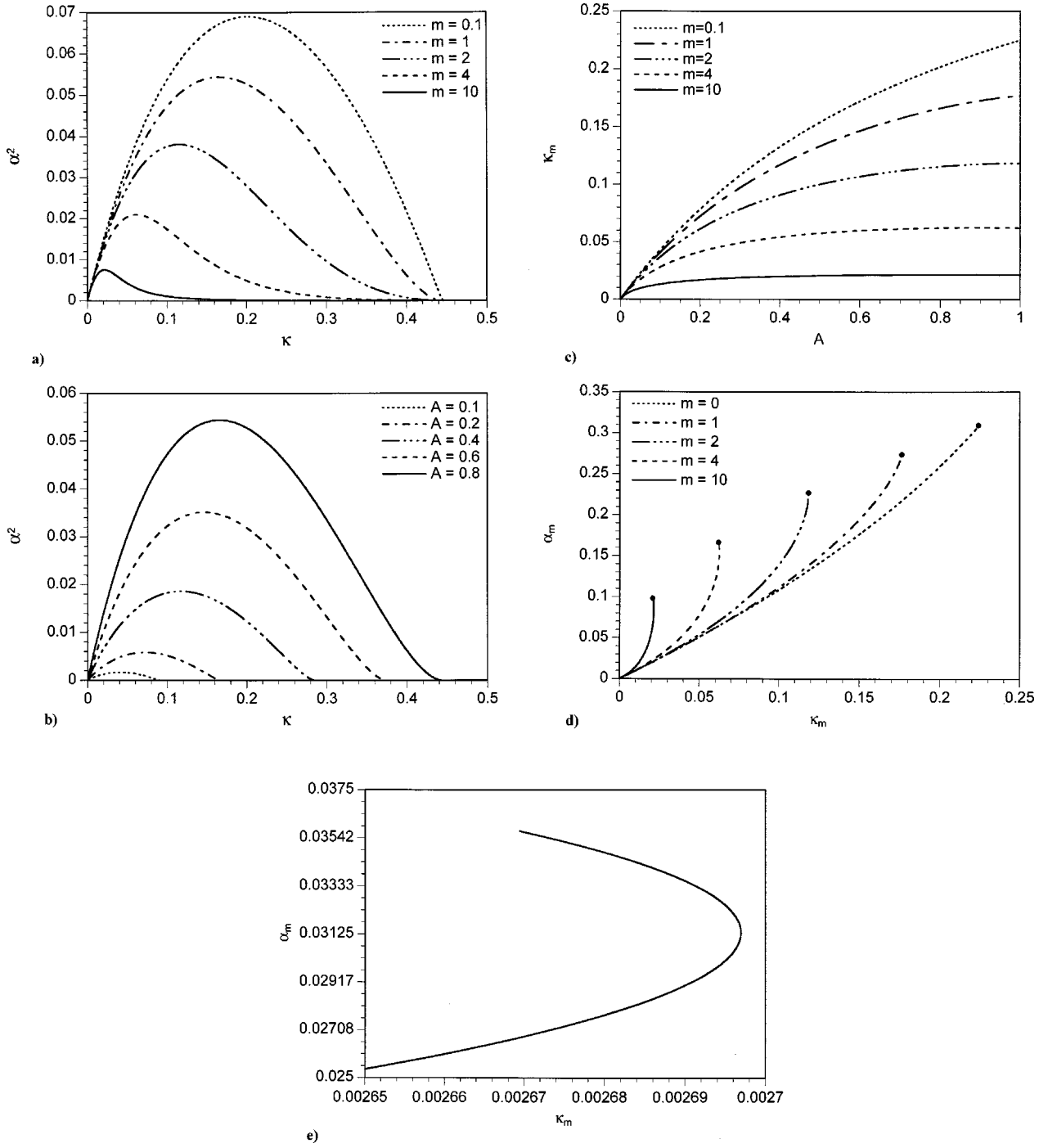

FIG. 3. For solid/fluid interfaces, variation of α^2 as a function of κ (a) for $A=0.8$ and different values of m: ·····, $m=0.1$; –·–·–·–, $m=1$; —···—, $m=2$; - - - - - -, $m=4$; —, $m=10$; (b) for $m=1$ and different values of A: ·····, $A=0.1$; –·–·–·—, $A=0.2$; —···—, $A=0.4$; - - - - - -, $A=0.6$; —, $A=0.8$. Boundaries of the most unstable modes in the (c) κ_m-A plane for different values of m: ·····, $m=0.1$; –·–·–·–, $m=1$; —···—, $m=2$; - - - - -, $m=4$; —, $m=10$; (d) α_m-κ_m plane for different values of m: ·····, $m=0$; –·–·–·–, $m=1$; —···—, $m=2$; - - - - - -, $m=4$; —, $m=10$; (e) locus of the double-valued region in the α_m-κ_m plane for $m=50$.

For a solid/solid interface, with a fixed $A(=0.8)$, Fig. 4(a) shows α^2 as a function of κ for increasing values of the shear moduli ratio $R[=(G_1/G_2)^{1/2}]$ as obtained from the physically meaningful solutions of Eq. (29). In this case, the κ_c continuously decreases as R increases and the topology of the growth rate curves is similar for all R (the slope of the curve at the interception with the abscissa is weakly dependent on the value of R). In fact, these curves are nearly self-similar if the ordinate and the abscissa are scaled by α/α_m and κ/κ_c, respectively. Clearly, the increase in strength in the lighter solid layer stabilizes the interface, requiring longer wavelengths for instability. For a fixed $R(=0.5)$, Fig. 4(b) shows that the behavior of α_m^2 as A decreases is very similar to that in Fig. 1(a) for $m=0$ (except for the smaller values of α_m^2).

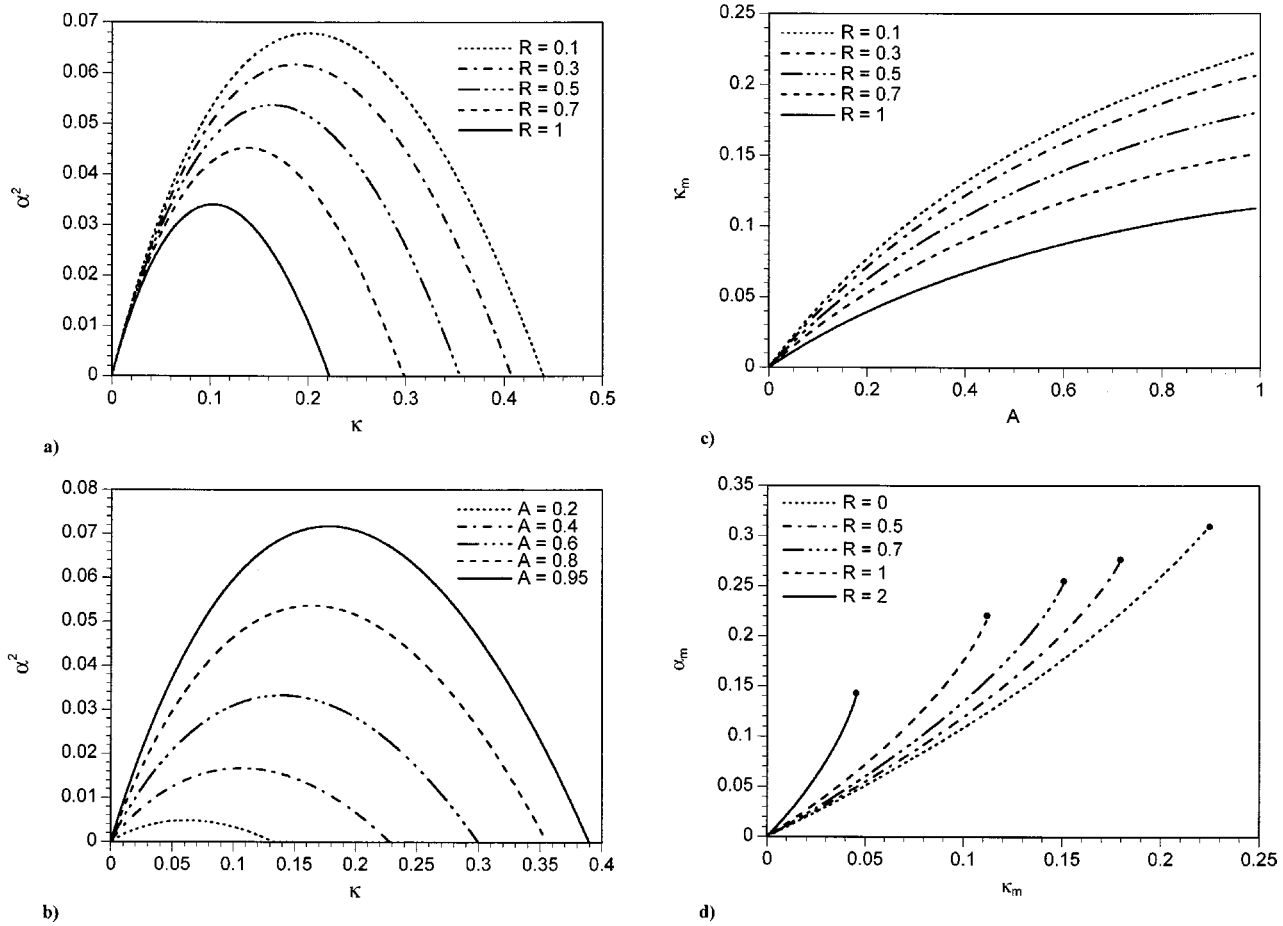

FIG. 4. For solid/solid interfaces, variation of α^2 as a function of κ (a) for $A=0.8$ and different values of R: ·····, $R=0.1$; –·–·–·–, $R=0.3$; —···—, $R=0.5$; - - - - - -, $R=0.7$; —, $R=1$; (b) for $R=0.5$ and different values of A: ·····, $A=0.2$; –·–·–·—, $A=0.4$; —···—, $A=0.6$; - - - - -, $A=0.8$; —, $A=0.95$. Boundaries for the most unstable modes in the (c) κ_m-A plane for different values of R: ·····, $R=0.1$; –·–·–·–, $R=0.3$; —···—, $R=0.5$; - - - -, $R=0.7$; —, $R=1$; (d) α_m, κ_m plane for different values of R: ·····, $R=0$; –·–·–·–, $R=0.5$; —···—, $R=0.7$; - - - - -, $R=1$; —, $R=2$.

Figure 4(c) shows the monotonic increase of κ_m with A for different values of R. For small R, these curves are similar to those in Fig. 3(c) for small m. However, as R increases, the slopes $(\partial\kappa_m/\partial A)$ of curves with small A are smaller than those seen in Fig. 3(c) with large M, and the converse is true for curves corresponding to values of A near unity. Finally, Fig. 4(d) shows the locus of the most unstable α_m-κ_m pairs for all A and different R. Unlike the behavior found in solid/fluid interfaces, these curves are single-valued for all R.

V. CONCLUDING REMARKS

For initially planar solid/fluid and solid/solid interfaces, we derived dispersion relations from which we computed the stability boundaries and loci of the most unstable modes (a condition attained for all wavelengths whose growth rates are maxima) in dimensionless space spanning the entire range of driving conditions. We showed that both kinds of interfaces could only become unstable via steady onset (oscillatory onset is not admissible). At accelerated perfectly planar solid/fluid and solid/solid interfaces, the selected wavelength takes place within the elastic regime of the solid media and corresponds to the most unstable mode for the particular configuration.

The simplifying assumptions that allowed an analytic treatment for the present linear stability analyses at solid/fluid and solid/solid interfaces are constant acceleration, incompressible media, isothermal conditions, infinite thickness, and a single wavelength. Even though these assumptions do not apply to a magnetically imploding smooth metal liner [19,20] that is continuously accelerated, the material is compressible, and the mechanical properties and thermodynamic state change in space and time due to temperature gradients, inferences about the behavior of specific snapshots of the liner implosion can be made. From the dispersion relation for a liquid/vacuum interface [24], it can be shown that the most unstable wavelength and corresponding growth rate are

$$\lambda_{mf} = 12.805\left(\frac{\mu^2}{a\rho^2}\right)^{1/3}, \quad \sigma_{mf} = 0.46\left(\frac{a^2\rho}{\mu}\right)^{1/3}. \qquad (34)$$

Using Eqs. (34) with a mean acceleration of $5\times10^8 \mathrm{m/s^2}$ [20], a melt density of 2340 $\mathrm{kg/m^3}$, and the viscosity of molten aluminum, which is on the order of 1 mPa s [27],

results in $\sigma_{mf}=3.9\times10^{7}\mathrm{s}^{-1}$ (i.e., it would have taken only 1 ns for a disturbance of 10 μm in amplitude to grow larger than 0.5 mm) and $\lambda_{mf}=0.9$ μm, which is about 500 times larger than the experimental value of 0.5 mm for a nominally smooth liner [20]. These large discrepancies in λ and σ might be explained if the unstable wavelength selection process and instability growth were to occur while the liner is in solid rather than in liquid phase. From Eqs. (20) and (21), it can be shown that at a solid/vacuum interface, the most unstable wavelength and growth rate are

$$\lambda_{ms}=27.85\frac{G}{a\rho},\quad \sigma_{ms}=0.31a\left(\frac{\rho}{G}\right)^{1/2}. \tag{35}$$

The spatiotemporal variation of the liner shear modulus is dictated by its thermodynamic state during implosion, and the magnitude of this modulus can be estimated, for instance, by the Steinberg-Cochran-Guinan constitutive equation [28]. From the temperature, density, and pressure histories in the implosion experiments [20], it is possible to reach a state in which the liner has softened to $G=21$ MPa, with a density of 2345 $\mathrm{kg/m}^3$ (slightly higher than at the melting point). Under these conditions, Eqs. (35) yield $\lambda_{ms}=0.5$ mm and $\sigma_{ms}=1.7\times10^{6}\mathrm{s}^{-1}$ [since $h\approx4\lambda_{ms}$, Eqs. (35) are applicable]. A disturbance with amplitude of 10 μm would grow to about 0.5 mm in 2.4 μs, which is more in line with experiments [20].

In magnetically imploded liners, the driving conditions that can destabilize the system are continuously changing in space and time. As shown in the Atlas experiments for smooth liners [20], there is a time interval of stable states. At the beginning of implosion, the shear modulus of the liner is high, the acceleration is low, and thus the most unstable wavelength is larger than any characteristic length scale. As implosion progresses, the liner could reach a potentially unstable state at a low growth rate incapable of destabilizing disturbances within the experimental time scale. Subsequently, the combined effect of a continuously decreasing shear modulus (due to Ohmic heating) with the increasing acceleration of the liner could lead to a sufficiently high growth rate to enable instability. Therefore, during the evolution of the implosion process of a nominally smooth liner, several potentially unstable states are passed over until a state is reached that has a sufficiently high growth rate and an admissible wavelength (with respect to the liner dimensions) to destabilize the interface before melting. We suggest that for nominally smooth imploding liners, wavelength selection is determined by the most unstable mode when the liner is in the solid phase. Once this wavelength is selected within the elastic regime, it will carry over into the nonlinear plastic regime and into the early stages of fluid flow if melting occurs.

The growth rate of a disturbance is expected to change beyond the elastic limit of the solid. However, little is known about disturbance growth rates in the plastic regime [10], and a compelling theoretical treatment has yet to be developed. Recently, Colvin *et al.* [29] performed simulations and developed an approximate analytical model to estimate the growth rate of instabilities in elastoplastic media. Their dispersion relation [Eq. (7) in Ref. [29]] for $A=1$ predicts a cutoff wavelength λ_c of $2\pi G/a\rho$ that is off by a factor of 2 from the correct result of $4\pi G/a\rho$ (for $h>\lambda/2$) first obtained by BK, confirmed by PS, and rigorously derived and generalized in this paper (also, these authors misquoted Miles' result for $\lambda_c=13\pi G/2a\rho$ [3]). Consequently, their dispersion relation leads to the incorrect most unstable wavelength within the elastic regime, and even though they account for the layer thickness h, their λ_c is independent of h (for very thin layers $\lambda_c\sim h^{1/2}$ as shown earlier [9,11,15,16]).

ACKNOWLEDGMENTS

The author thanks G. Dimonte and R. Keinigs for stimulating discussions, and an anonymous reviewer for valuable comments. Los Alamos National Laboratory is operated by the University of California for the U.S. Department of Energy under Contract W-7405-ENG-36.

[1] D. H. Sharp, Physica D **12**, 3 (1984).
[2] H. J. Kull, Phys. Rep. **206**, 197 (1991).
[3] J. W. Miles, General Dynamics Report No. GAMD-7335, AD643161, 1966 (unpublished).
[4] G. N. White, Los Alamos National Laboratory Report LA-5225, 1973 (unpublished).
[5] A. C. Robinson and J. W. Swegle, J. Appl. Phys. **66**, 2859 (1989).
[6] E. L. Ruden and D. E. Bell, J. Appl. Phys. **82**, 163 (1997).
[7] S. M. Bakhrakh and N. P. Kovalev, *Proceedings of the 5th All-Union Conference on Numerical Methods for the Solution of Elasticity and Plasticity Theory Problems*, Novosibirsk, 1978, pp. 15–23 (in Russian).
[8] S. M. Bakhrakh and N. P. Kovalev, *Numerical Methods for Solid State Mechanics*, Novosibirsk, 1980, Vol. 2, pp. 5–21 (in Russian).
[9] S. M. Bakhrakh, O. B. Drennov, N. P. Kovalev, A. I. Lebedev, E. E. Meshkov, A. L. Mikhailov, N. V. Nevmerzhitsky, P. N. Nizovtsev, V. A. Rayevsky, G. P. Simonov, V. P. Solovyev, and I. G. Zhidov, Lawrence Livermore National Laboratory Report No. UCRL-CR-126710, 1997 (unpublished)
[10] D. C. Drucker, *Mechanics Today*, edited by S. Nemat-Nasser (Permagon, Oxford, 1980), Vol. 5, p. 37.
[11] P. N. Nizovtsev and V. A. Raevskii, VANT Ser. Teor. Prikl. Fiz. **3**, 11 (1991) (in Russian).
[12] J. W. Swegle and A. C. Robinson, J. Appl. Phys. **66**, 2838 (1989).
[13] J. F. Barnes, P. J. Blewett, R. G. McQueen, K. A. Meyer, and D. Venable, J. Appl. Phys. **45**, 727 (1974); **51**, 4678 (1980).
[14] A. I. Lebedev, P. N. Nizovtsev, V. A. Raevskii, and V. P. Solov'ev, Phys. Dokl. **41**, 328 (1996).
[15] A. I. Lebedev, P. N. Nisovtsev, and V. A. Rayevsky,

Rayleigh-Taylor Instability in Solids, in *Proceedings of the Fourth International Workshop on the Physics of Compressible Turbulent Mixing*, edited by P. F. Linden, D. L. Youngs, and S. B. Dalziel (Cambridge University Press, Cambridge, 1993), pp. 81–93.
[16] B. Plohr and D. H. Sharp, ZAMP **49**, 786 (1998).
[17] G. Dimonte, Phys. Plasmas **6**, 2009 (1999).
[18] G. Dimonte, R. Gore, and M. Schneider, Phys. Rev. Lett. **80**, 1212 (1998).
[19] R. K. Keinigs, W. L. Atchison, R. J. Faehl, V. A. Thomas, K. D. Mclenithan, and R. J. Trainor, J. Appl. Phys. **85**, 7626 (1999).
[20] R. E. Reinovsky, W. E. Anderson, W. L. Atchison, C. E. Ekdahl, R. J. Faehl, I. R. Lindemuth, D. V. Morgan, M. Murillo, J. L. Stokes, and J. S. Shlachter, IEEE Trans. Plasma Sci. **30**, 1764 (2002).
[21] R. L. Bowers, J. H. Brownell, H. Lee, K. D. McLenithan, A. J. Scannapieco, and W. R. Shanahan, J. Appl. Phys. **83**, 4146 (1998).
[22] H. W. Turnbull, *Theory of Equations* (Oliver and Boyd, Edinburgh, 1952).
[23] D. Wang, *Elimination Methods* (Springer-Verlag, Vienna, 2001).
[24] S. Chandrasekhar, *Hydrodynamic and Hydromagnetic Stability* (Oxford University Press, London, 1968).
[25] K. O. Mikaelian, Phys. Rev. E **54**, 3676 (1996).
[26] R. Menikoff, R. Mjolsness, D. Sharp, C. Zemach, and B. Doyle, Phys. Fluids **21**, 1674 (1978).
[27] T. Iida and R. I. L. Guthrie, *The Physical Properties of Liquid Metals* (Clarendon Press, Oxford, 1988).
[28] D. J. Steinberg, S. G. Cochran, and M. W. Guinan, J. Appl. Phys. **51**, 1498 (1980).
[29] J. D. Colvin, M. Legrand, B. A. Remington, G. Schurtz, and S. V. Weber, J. Appl. Phys. **93**, 5287 (2003).